Journal of Hazardous Materials 274 (2014) 455–464

Contents lists available at ScienceDirect

Journal of Hazardous Materials

journal homepage: www.elsevier.com/locate/jhazmat

# Chemometric approach to visualize and easily interpret data from sequential extraction procedures applied to sediment samples

Mónica B. Alvarez[a,*], Pamela Y. Quintas[b], Claudia E. Domini[a], Mariano Garrido[a], Beatriz S. Fernández Band[a]

[a] Instituto de Química del Sur, INQUISUR (UNS-CONICET), Av. Alem 1253, B8000CPB Bahía Blanca, Buenos Aires, Argentina
[b] Marine Chemistry Laboratory, IADO (UNS-CONICET), Florida 8000, B8000FWB, Bahía Blanca, Buenos Aires, Argentina

## HIGHLIGHTS

- Two sequential schemes discriminating different oxide phases were used.
- Tucker4 model made possible to visualize and explain the data set information.
- Although different, the 2 sequential procedures used give similar information.
- Metal mobility/availability was assessed for estuarine sediment samples.

## ARTICLE INFO

*Article history:*
Received 6 November 2013
Received in revised form 25 March 2014
Accepted 20 April 2014
Available online 26 April 2014

*Keywords:*
Four-way Tucker model
Metal fractionation
Oxide phases
Sediment samples
Sequential extraction procedures

## ABSTRACT

The aim of this study was to assess metal mobility/availability in coastal surface (oxic) sediment samples from the Bahía Blanca estuary. Particularly, two sequential extraction procedures able to discriminate metals associated to amorphous Fe and Mn oxides and those associated with crystalline oxides of Fe were applied. Sequential procedures differ in the number of steps, type of reagents used, and in the order in which metals associated to organic matter are extracted. The studied metals were Cd, Cr, Cu, Pb, Ni and Zn because of their hazardous potential and relative abundance in the estuary. Tucker4 model with three factors describes appropriately the data sets (explained variance of 64.05%). This model made it possible to visualize and explain the information underlying in the data set. From the multivariate analysis, it was possible to evaluate the metal behaviour and their availability. In this way, Cd and Zn are associated to the more available fractions whereas Ni, Cr, Cu and Pb are mainly associated to the unavailable fractions. On the other hand, Zn and Cu are associated to organic matter fraction. Despite the fact that the two-fractionation schemes are quite different, the results obtained with both schemes are comparable.



## 1. Introduction

Sediments are constituted by fragments derived from soils and rocks, biological materials and other contributions of anthropogenic origin. Conditions of the aquatic environment, critically affect the chemical characteristics of the sediments. Sediments can act as sinks or sources of heavy metals depending on their geochemical composition and changes in the physicochemical conditions, i.e. pH, presence of organic chelates, redox potential, dissolved oxygen, etc. [1,2].

Heavy metals may be associated to several solid phases in the sediments, i.e. clays, organic matter, oxides, carbonates, sulphides and residual silicates, which are mutually interrelated [1–3]. Heavy metals are adsorbed on the surface of clay particles and are also occluded in amorphous materials such as Fe and Mn oxyhydroxides, sulphides and organic matter that can act as coatings of other sediment particles. They also take part of the crystalline lattice of primary minerals such as residual silicates [4].

Currently it is normally accepted that total metal concentration gives less information about the metal behaviour than fractionation analyses [1]. The fractionation methods consist of extraction/lixiviation procedures carried out under operationally defined conditions. The term 'operational' is established to indicate that metal concentrations obtained in each fraction depend on the used experimental procedure [5–7]. Most widely used chemical

* Corresponding author. Tel.: +54 2914595100; fax: +54 2914595160.
*E-mail addresses:* malvarez@criba.edu.ar, monica.alvarez@uns.edu.ar (M.B. Alvarez).

http://dx.doi.org/10.1016/j.jhazmat.2014.04.039
0304-3894/

extractants are classified as inert electrolytes, weak acids, reducing and oxidizing agents, complexing reagents and strong acids. The aim of a particular fractionation study determines the appropriate sequence of reagents to obtain the required partitioning degree (number of steps). These procedures are based on selecting different reagents with increasing dissolving power respect to the geochemical phases. The relative solubility of metal species associated to a particular geochemical phase depends on the degree of reagent's dissolving power [8]. In this sense, there are traditional sequential extraction schemes described in the literature [6,9–12] and others recently reported [13–16].

In the last decades, Fe and Mn oxyhydroxide phases have received major attention because of their significant role in the heavy metal fixation. This is reflected in the application of sequential schemes tending to discriminate the metals associated to the Fe/Mn amorphous oxides and the Fe crystalline oxides [4,17–19]. These schemes are based on the different behaviours of Mn and Fe oxyhydroxides under various redox potential and pH conditions [20,21]. The most effective mixture of reagents to assess the metals associated to these phases contains both a reducing and a chelating agent able to keep the released metals in a soluble form.

These kinds of studies are particularly important in well-mixed estuaries. In such closed environments, sediments take a long time until they are deposited near the shore; therefore, physicochemical processes have enough time to occur [3]. The Bahía Blanca estuary (Buenos Aires, Argentina) is a case study of this type of closed environment, which is particularly interesting because it possesses a deep-water port (45 feet) requiring periodic dredging. This practice leads to a large movement of sediments that could derive in a potential risk of pollution. The high turbidity is an important characteristic of the system, caused mainly by an intense tidal regime and prevailing strong N and NW wind which generate water mixing and re-suspension phenomena [22,23]. Furthermore, the estuary receives water from fresh water streams and passes through important agricultural and ranching areas.

Environmental data originated in fractionation studies give rise to large multivariate arrays. They require variable reduction techniques to provide an easy visualization and interpretation of the information hidden in the data set. The obtained data show a multidimensional structure (samples, metals, fractions, extraction procedures) and could be analyzed using a four-way multivariate chemometric tools such as PARAFAC and Tucker models [24–27]. This kind of data could be rearranged in partial data sets with lower dimensions and analyzed by a simpler method such as PCA [28]. However, this approach does not have the ability of dealing with the whole data set in a unique analysis [29,30].

The goal of this study was to assess the availability and behaviour of heavy metals associated to different solid phases of sediment samples of the Bahía Estuary. To this aim, two sequential extraction schemes [10,11] were applied to oxic sediment samples from the Bahía Blanca estuary. The fractionation procedures vary in the number of steps. They also differ in the order in which organic matter and oxide phases are extracted. Cd, Cr, Cu, Pb, Ni and Zn were studied, either because of their hazardous potential or relative abundance in the estuary (probably associated with industrial activities) [26,27]. A better visualization of the results was obtained using a Tucker4 model. The choice of Tucker instead of PARAFAC (a particular case of Tucker) was based on the ability of Tucker of handle different number of factors in each mode, which make it possible to extract more information. In addition, one collateral scope of this study is to qualitatively corroborate that the results obtained by the two different sequential extraction schemes (using different reagents, temperature, and extraction times) are equivalent.

## 2. Experimental

### 2.1. Reagents and solutions

All chemicals and reagents were of analytical reagent grade. Doubly distilled demineralized water was used throughout. Before use all containers were soaked in 15% $HNO_3$ for 24 h, and rinse with doubly distilled water. Carlo Erba (Erbatron RSE, Milan, Italy) HF, HCl and $HNO_3$ were used. Stock solutions of the analytes (1000 mg $L^{-1}$) were obtained from Carlo Erba Normex Standards (Milan, Italy). Multielement standard solutions were prepared by diluting suitable volumes of the stock solutions with 0.5 mol $L^{-1}$ $HNO_3$. A solution for Cr was prepared to avoid the instability of the signals observed when this element was included in the multielemental solution [31].

In order to assess the total metal concentrations, Antarctic bottom sediment (MURST-ISS-A1, provided by Italian Research Program in Antarctica) certified for total metal concentrations was used. The total metal concentration was assessed following the procedure stated in [27]. X-ray diffraction analysis showed that the mineral constitution of the Antarctic sediment resembles, in a global way, the composition of the coastal sediments studied (quartz, feldspars such as anorthite and albite, carbonates, iron oxides and hydroxides) [31].

### 2.2. Study area

The Bahía Blanca estuary is located in the south of the Buenos Aires Province, Argentina, (38°46′S, 62°30′W) and has a northwest-southeast direction (Fig. 1). Several fresh water streams flow into the north of the main channel, which is primarily sailed by fishing boats and cargo vessels (generally carrying fuel and cereals). Three urban nucleuses are located in the northern coast of the estuary. The largest of them is Bahía Blanca city, with a population exceeding 300,000 inhabitants. The southern coast is not well defined and varies with the tides.

This area constitutes a big industrial emplacement, composed by refineries, petrochemical industries and fertilizer manufacturers. Moreover, there are textile and tannery industries that coexist with cereal and meat factories. Pollutants reach the estuary through the different sources of fresh water carrying direct industrial discharges and municipal wastewater.

### 2.3. Sampling and sample treatment

The sampling zone is characterized by the presence of fine sand, silt and clay surface sediments. Eight samples (S1 to S8) were collected in the Galván port area (about 5 ha in surface) because of the proximity to important industries, i.e. the main sources of pollution (see Fig. 1). Several portions were collected along a zig-zag track [32], in the same sampling point, in order to obtain representative composite samples. Surface oxic sediment samples (light brown colour, flaky appearance, no sulphide smell) were taken from the superficial layer (1–5 cm) using a plastic spatula. The samples were kept at 4 °C before analysis.

Samples were air-dried for at least 72 h and sieved (250 mesh). The lower particle size fraction (<63 μm) was retained.

### 2.4. Procedure

The classical extraction schemes [6,9] consider metals linked to oxides as a unique phase (named "oxides of Fe and Mn"). By contrast, the selected sequential extraction procedures for our study are able to discriminate between metals associated to the phase comprised by Mn oxides and amorphous Fe oxyhydroxides and those adsorbed on crystalline Fe oxides [10,11]. Amorphous iron

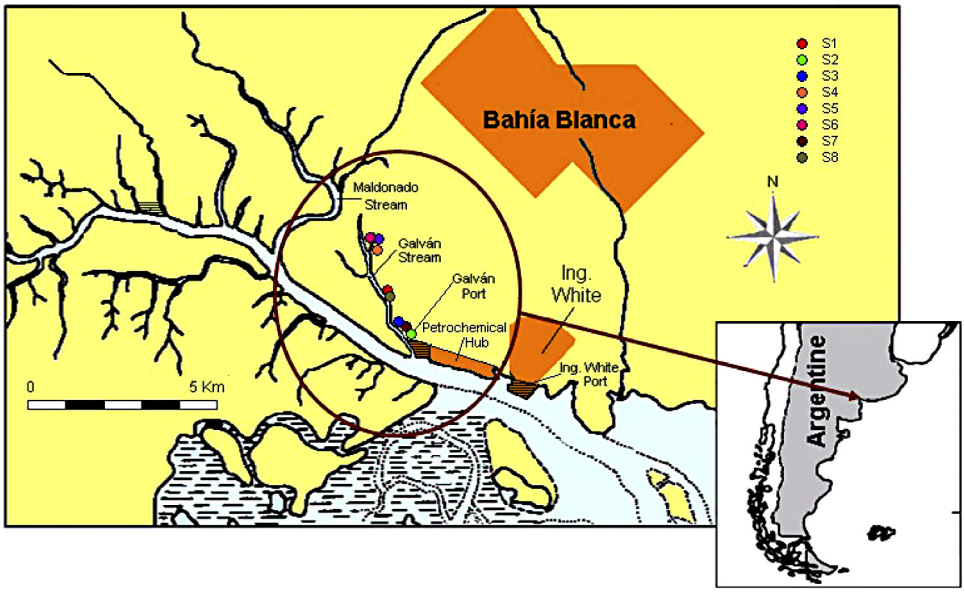


**Fig. 1.** Map showing the study area and the sampling points.

oxyhydroxides and manganese oxides form mixed oxides because of their similar chemical properties and ionic radii. They are chemically more reactive than crystalline Fe oxides and it is on this basis that metals associated to these different phases (amorphous and crystalline) are separated [11]. It is remarkable that extraction conditions for metals linked to amorphous oxyhydroxide phase are relatively independent of pH (it could vary from 1 to 3), concentration of the reducing agent (0.025 to 0.25 mol $L^{-1}$ $NH_2OH{\cdot}HCl$) and extraction time (15–60 min) [20]. Furthermore, the extraction of metals associated to crystalline Fe oxides needs stronger conditions (lower pH, higher reducing agent concentration, longer extraction time and higher temperature).

The successive chemical extraction steps and volumes of reagents involved in the sequential extraction schemes used in our work are summarized in Fig. 2. The fractionation Scheme 1, consisting of seven steps was adapted from the procedure reported by Gupta and Chen [10]. The fractionation Scheme 2 comprises five steps and was an adaptation of the procedure proposed by Hall et al. [11].

All the operations were performed in 50 mL polypropylene centrifuge tubes provided with screw stoppers, except the last step (in both procedures) which was carried out in PTFE vessels. The initial mass of sediment was 2.000 ± 0.001 g. The extracts were separated from the solid residue by centrifugation at 3000 rpm (1006 × *g*) for 30 min. The residue was washed once with 10.0 mL of water and the washings discarded before continuing the extraction sequence. The final solution volume was 25.0 mL. Four procedural replicates for the same sample were prepared for each scheme. Blanks for all stages of each procedure were prepared as well.

Flame atomic absorption measurements were performed with a Perkin-Elmer AAnalyst 200 spectrometer equipped with single element hollow cathode lamps for Cr, Cu, Ni and Pb. For Cd and Zn electrodeless discharge lamps were used. The spectrometer was operated at maximum sensitivity with air/acetylene flame. Analytical wavelengths (nm) were Cd: 228.8, Cr: 359.3, Cu: 324.8, Ni: 341.5, Pb: 283.3 and Zn: 213.9. Determination limits for the atomic spectrometric procedure were estimated from solutions containing the matrix components, ie. simulating the composition of the solutions from each extraction step. Practical values were calculated as three times the IUPAC detection limit (LOD), defined as the ratio between three times the standard deviation of the blank signal (for $n = 10$) and the slope of the calibration line.

### 2.5. Multivariate analysis

The data were arranged in a multi-way array $\underline{\mathbf{X}}$ ($I \times J \times K \times L$) ($I$ corresponds to the number of samples analyzed, $J$ is the number of metals studied, $K$ consists of the number of fractions established in each fractionation scheme, and $L$ is the number of sequential extraction schemes simultaneously examined). Scaling within the metals mode ($J$-mode) was carried out in order to ensure that metals have the same possibility to contribute to the model [24]. This eliminates the differences among metals arising from their different magnitudes, while retaining the differences among the sampling sites, fractions and schemes.

In accordance with the multi-way structure of the data set, a method able to deal with four-way data has been applied. Tucker4 model [29] decomposes the four-way data array $\underline{\mathbf{X}}$ into four loading matrices $\mathbf{A}$ ($I \times P$), $\mathbf{B}$ ($J \times Q$), $\mathbf{C}$ ($K \times R$) and $\mathbf{D}$ ($L \times S$), where $P$, $Q$, $R$ and $S$ are the number of factors in each mode, as follows:

$$\underline{\mathbf{X}} = \sum_{p=1}^{P}\sum_{q=1}^{Q}\sum_{r=1}^{R}\sum_{s=1}^{S} a_{ip} b_{jq} c_{kr} d_{ls} g_{pqrs} + e_{ijkl} \quad (1)$$

In Eq. (1), $e_{ijkl}$ corresponds to each residual element in the $\underline{\mathbf{E}}$ ($I \times J \times K \times L$) array and the $g_{pqrs}$ are the elements from the four-way core array $\underline{\mathbf{G}}$ ($P \times Q \times R \times S$). Tucker4 model was chosen because it enabled the selection of different number of factors in each mode. This is particularly helpful in the current data set, in which the fourth mode has only two schemes. In addition, Tucker4 gives the core array $\underline{\mathbf{G}}$, which contains information about the interactions among the loading vectors in the different modes [30]. Since Tucker models have rotational freedom, we rotated the core in order to maximize the explained variance with fewer factor combinations. For such a rotated core, the loadings were counter-rotated so that the model of the data was still the same [30].

The optimal model was selected using the numerical convex-hull-based method proposed by Ceulemans and Kiers [33], with the st-criterion —defined on the basis of residual sum of squares and the degrees of freedom (d.f.) [25,34]. Instead of the goodness-of-fit used in the original work. An explanation of st-coefficients computation can be found elsewhere [25]. Thus, the model with largest st-coefficient was selected. Multi-way modelling was performed using N-way Toolbox [35] in Matlab 7.0 (The MathWorks).

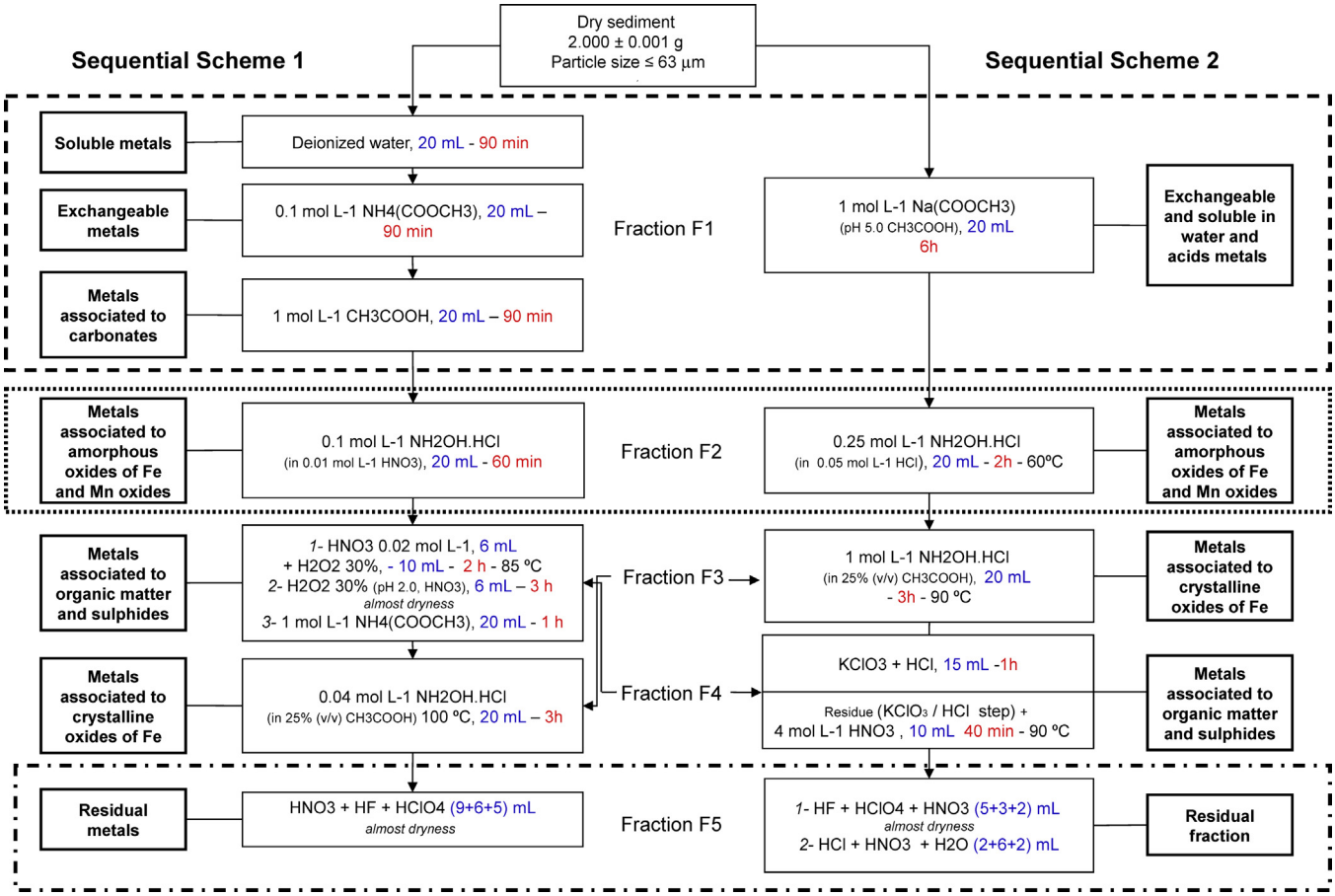


**Fig. 2.** Flow chart comparing the two sequential extraction schemes.

## 3. Results and discussion

### 3.1. Sequential extraction schemes

The results from the applied sequential extraction procedures are summarized in Tables 1 and 2. Repeatability is indicated as the confidence interval with 95% confidence level, obtained for 4 determinations. The resulting precision may be regarded as acceptable considering the substantial number of manipulations applied in the sequential schemes.

Fig. 3 shows bar charts that display the distribution patterns with metal proportions associated with each fraction. In general, a good correlation is observed between the two fractionation schemes, despite the differences in the number of steps and the order of extraction of organic matter fraction. In order to verify the reliability and consistency of the results obtained by the two sequential extraction procedures, the recoveries based on the total metal concentration were calculated (Table 3). Recoveries were acceptable and ranged between 86.0 and 108.0% for the studied samples and between 95.8 and 109.0% for the reference material.

The sum of the first three steps of sequential extraction Scheme 1 (Table 1, soluble metals, exchangeable metals and those associated to carbonates) is comparable to the first step of sequential extraction Scheme 2 (Table 2, exchangeable and soluble in water and acids metals). Moreover, this procedure was corroborated by comparing these results with the ones obtained by BCR protocol (published in [26]) for samples S7 and S8 and for the reference material MURST-ISS-A1. The results were statistically comparable ($\alpha = 0.05$).

### 3.2. Multi-way analysis interpretation

When many samples are submitted to different sequential extraction schemes that give various fractions, in which several metals are determined, the amount of data obtained could be significantly high. So, obtaining and explaining relevant information by a simple inspection or interpretation of data tables or bar charts (Fig. 3) become a complex task. However, this kind of data intrinsically has a multi-way structure and could be analyzed by multi-way methods. These methods are more adequate to carry out the so-called 'data mining', whose overall goal is to extract information from a data set and transform it into an understandable structure for further use. Multi-way methods such as PARAFAC (Parallel Factor Analysis) [30] compel the model to have the same number of factors for all the modes. In the current data set, which has only two sequential schemes in the fourth mode, using PARAFAC could be a drawback. So, the selected multi-way method was Tucker4, because of its ability to work with different number of factors in each mode.

The first step in the Tucker4 analysis was the selection of the optimal model complexity. Generally, the optimal complexity of the Tucker model is the one retaining the maximum data variance using the smallest number of components. In this study we used the Ceulemans–Kiers st-criterion [33] to determine the optimal model complexity. With this purpose, the plot of explained data variance versus model complexity ($P \times Q \times R \times S$) was carried out (Fig. 4). The st-criterion was applied only for the seven models lying in the upper boundary of the convex-hull (Fig. 4). Table 4 shows the corresponding st-coefficients. Although the variance explained by the model has quite low values, it is in agreement with the characteristic of

**Table 1**
Concentration of metals (±confidence interval, $n = 4$, $\alpha = 0.05$) in mg kg$^{-1}$ (dry basis) for fractionation Scheme 1.

| | Cd | Cr | Cu | Ni | Pb | Zn |
|---|---|---|---|---|---|---|
| Fraction 1 (step 1 + 2 + 3) | | | | | | |
| S1 | 0.65 ± 0.04 | <0.65 | 12.15 ± 0.59 | <0.65 | 4.12 ± 0.38 | 103 ± 5 |
| S2 | 0.67 ± 0.04 | <0.65 | 6.33 ± 0.26 | <0.65 | 6.00 ± 0.52 | 59.05 ± 4.48 |
| S3 | 0.70 ± 0.06 | <0.65 | 6.91 ± 0.25 | 3.28 ± 0.24 | 5.12 ± 0.44 | 25.22 ± 2.19 |
| S4 | 0.55 ± 0.06 | <0.65 | 15.35 ± 0.68 | <0.65 | 5.05 ± 0.40 | 45.94 ± 3.63 |
| S5 | 1.60 ± 0.08 | <0.65 | 9.91 ± 0.54 | 4.35 ± 0.32 | 3.38 ± 0.25 | 15.55 ± 0.98 |
| S6 | 1.02 ± 0.07 | <0.65 | 11.65 ± 1.05 | 3.25 ± 0.29 | <1.70 | 65.86 ± 4.95 |
| S7 | 1.17 ± 0.09 | <0.65 | <0.75 | <0.65 | 6.84 ± 0.55 | 14.52 ± 0.96 |
| S8 | 0.90 ± 0.06 | <0.65 | 13.71 ± 0.48 | <0.65 | <1.70 | 211 ± 16 |
| MURST-ISS-A1 | 0.49 ± 0.04 | <0.65 | <0.75 | <0.65 | <1.70 | 6.29 ± 0.42 |
| Fraction 2 (step 4) | | | | | | |
| S1 | 0.25 ± 0.02 | 3.05 ± 0.18 | 3.08 ± 0.15 | 5.25 ± 0.48 | 5.45 ± 0.44 | 86.50 ± 7.95 |
| S2 | 0.29 ± 0.03 | 1.92 ± 0.10 | 5.45 ± 0.22 | 3.65 ± 0.35 | 7.55 ± 0.68 | 14.33 ± 1.22 |
| S3 | 1.13 ± 0.08 | 4.65 ± 0.25 | 11.15 ± 0.95 | 6.65 ± 0.62 | 14.10 ± 1.12 | 20.25 ± 1.86 |
| S4 | 0.36 ± 0.03 | 3.45 ± 0.22 | 9.98 ± 0.68 | 8.52 ± 0.76 | 10.33 ± 0.97 | 14.63 ± 1.31 |
| S5 | 0.39 ± 0.04 | < 0.65 | 12.55 ± 0.81 | 7.10 ± 0.65 | 20.32 ± 1.75 | 25.65 ± 1.93 |
| S6 | 1.25 ± 0.09 | 5.13 ± 0.28 | 13.33 ± 0.93 | 8.45 ± 0.78 | 4.45 ± 0.38 | 22.12 ± 1.85 |
| S7 | 0.78 ± 0.06 | 3.98 ± 0.22 | 9.75 ± 0.65 | 3.13 ± 0.28 | 14.36 ± 1.26 | 10.05 ± 0.98 |
| S8 | <0.10 | <0.65 | 3.50 ± 0.08 | 1.75 ± 0.24 | <1.70 | 62.50 ± 5.34 |
| MURST-ISS-A1 | <0.10 | <0.65 | <0.75 | <0.65 | <1.70 | 1.46 ± 0.13 |
| Fraction 3 (step 6) | | | | | | |
| S1 | 0.65 ± 0.05 | 3.75 ± 0.26 | 7.33 ± 0.58 | 3.85 ± 0.35 | 15.13 ± 1.33 | 42.25 ± 3.82 |
| S2 | 0.68 ± 0.04 | 4.30 ± 0.32 | 12.22 ± 1.02 | 10.12 ± 0.95 | 27.63 ± 2.46 | 45.53 ± 3.65 |
| S3 | 0.46 ± 0.03 | 15.13 ± 1.28 | 15.41 ± 1.11 | 7.85 ± 0.65 | 7.75 ± 0.70 | 37.38 ± 3.08 |
| S4 | 0.75 ± 0.06 | 14.53 ± 1.25 | 12.22 ± 1.08 | 7.08 ± 0.63 | 32.89 ± 3.02 | 65.75 ± 5.75 |
| S5 | 0.60 ± 0.05 | 12.85 ± 1.02 | 22.41 ± 1.95 | 5.65 ± 0.48 | 18.73 ± 1.66 | 37.38 ± 2.93 |
| S6 | 0.68 ± 0.06 | 12.45 ± 1.10 | 23.74 ± 1.87 | 8.75 ± 0.69 | 18.23 ± 1.75 | 56.30 ± 4.92 |
| S7 | <0.10 | <0.65 | 5.22 ± 0.45 | 2.68 ± 0.22 | 20.12 ± 1.88 | 45.15 ± 4.05 |
| S8 | <0.10 | 3.32 ± 0.25 | 7.04 ± 0.56 | 6.25 ± 0.54 | 5.13 ± 0.46 | 35.25 ± 3.13 |
| MURST-ISS-A1 | <0.10 | <0.65 | <0.75 | 0.80 ± 0.07 | <1.70 | <0.05 |
| Fraction 4 (step 5) | | | | | | |
| S1 | 0.63 ± 0.03 | 12.00 ± 1.05 | 40.25 ± 3.14 | 4.02 ± 0.31 | 15.31 ± 1.42 | 98.55 ± 8.33 |
| S2 | 0.60 ± 0.03 | 15.15 ± 1.24 | 23.11 ± 2.08 | 9.05 ± 0.82 | 12.43 ± 1.18 | 50.58 ± 4.95 |
| S3 | 0.65 ± 0.04 | 7.07 ± 0.63 | 25.44 ± 2.02 | 3.22 ± 0.25 | 7.43 ± 0.69 | 15.82 ± 1.28 |
| S4 | 0.63 ± 0.04 | 10.75 ± 0.95 | 21.11 ± 1.98 | 10.33 ± 0.96 | 12.92 ± 1.13 | 12.85 ± 0.95 |
| S5 | 0.48 ± 0.03 | 10.25 ± 0.98 | 17.44 ± 1.57 | 8.15 ± 0.69 | 10.05 ± 0.87 | 23.82 ± 1.84 |
| S6 | 0.55 ± 0.04 | 10.42 ± 0.86 | 9.42 ± 0.78 | 6.13 ± 0.42 | 5.33 ± 0.43 | 12.39 ± 0.75 |
| S7 | 0.64 ± 0.04 | <0.65 | 28.80 ± 2.25 | <0.65 | 15.10 ± 1.33 | 4.64 ± 0.39 |
| S8 | <0.10 | 14.00 ± 1.32 | 50.89 ± 4.76 | 4.33 ± 0.37 | 15.31 ± 1.25 | 175 ± 11 |
| MURST-ISS-A1 | <0.10 | 2.05 ± 0.16 | 4.07 ± 0.38 | 3.25 ± 0.20 | <1.70 | 4.73 ± 0.33 |
| Fraction 5 (step 7) | | | | | | |
| S1 | 0.95 ± 0.07 | 15.63 ± 1.12 | 20.45 ± 1.98 | 16.55 ± 1.25 | 11.83 ± 1.05 | 61.88 ± 5.42 |
| S2 | 1.05 ± 0.08 | 14.65 ± 1.03 | 27.44 ± 2.23 | 15.33 ± 1.13 | 12.18 ± 1.08 | 48.25 ± 4.55 |
| S3 | 0.83 ± 0.06 | 10.07 ± 0.94 | 19.82 ± 1.81 | 13.25 ± 1.06 | 11.95 ± 1.02 | 39.27 ± 3.83 |
| S4 | 1.22 ± 0.10 | 11.25 ± 1.05 | 27.44 ± 2.42 | 19.93 ± 1.69 | 9.96 ± 0.85 | 46.51 ± 4.36 |
| S5 | 0.95 ± 0.06 | 25.07 ± 2.25 | 39.82 ± 3.75 | 15.35 ± 1.08 | 24.95 ± 2.25 | 59.45 ± 5.69 |
| S6 | 1.36 ± 0.11 | 26.39 ± 2.33 | 18.83 ± 1.69 | 18.35 ± 1.35 | 13.63 ± 1.15 | 75.85 ± 6.98 |
| S7 | 0.65 ± 0.06 | 14.15 ± 1.08 | 32.03 ± 2.58 | 15.25 ± 1.09 | 14.52 ± 1.22 | 22.93 ± 1.88 |
| S8 | 0.29 ± 0.03 | 15.22 ± 1.10 | 22.12 ± 1.65 | 13.48 ± 1.03 | 4.96 ± 0.33 | 54.69 ± 4.93 |
| MURST-ISS-A1 | <0.10 | 40.97 ± 3.85 | 2.03 ± 0.17 | 5.76 ± 0.47 | 17.24 ± 1.58 | 40.68 ± 3.75 |

the samples, which have a composition resulting from both natural origin and variable anthropogenic inputs. As a result, the model with a complexity 3 × 3 × 3 × 1 was selected.

Five fractions (F1 to F5) were considered in order to compare the results obtained from the two fractionation schemes (Fig. 2).

Figs. 5a–c shows the loading plots for the *I*-mode (samples). When Factor 2 vs. Factor 1 plot is examined (Fig. 5a), it can be seen that almost all samples have similar and negative figures for Factor 1. Regarding Factor 2 S1, S8 and the reference material MURST-ISS-A1 have positive values and are clearly different from the other samples. Metals found in MURST-ISS-A1 are principally associated to the organic matter and residual fractions (Fig. 3, Tables 1 and 2). Moreover, samples S1 and S8 were collected in the proximity of an industrial effluent, and this area is characterized by high organic matter contents. Fig. 5b shows the Factor 3 vs. Factor 2 plot. MURST-ISS-A1 appears isolated from the other samples and has positive values for both factors. S1 and S8 samples have positive values for Factor 2 but exhibit negative values for Factor 3. On the other hand, a cluster involving S2, S4, S5 and S6 appears with negative values for both factors. Finally, S3 and S7 seem to be grouped showing negative values for Factor 2 and positive ones for Factor 3. Fairly, sample S7 and MURST-ISS-A1 exhibit the highest values for Factor 3. The same behaviour is observed in Fig. 5c, which displays a similar arrangement.

Loading plots for *J*-mode (metals) are depicted in Fig. 5d–f. In the plane formed by Factors 2 and 1, the metal distribution shows positive values for Factor 1 (Fig. 5d). Lower loading for Factor 1 seem to be related to the metals typically linked to F1, i.e. Zn, Cd and Pb to a lesser extent. On the contrary, the most positive values of Factor 1 would correspond to the less available metals. From another point of view, Factor 2 discriminates Zn and Cu from the other metals. An inspection of Tables 1 and 2 reveals that the metals mainly linked to organic matter fraction are Cu and Zn. Thus, Factor 2 seems to be related to the presence of Cu and Zn in the organic matter fraction. Several authors also reported associations of Cu to the organic matter fraction [8,18,36]. The amounts of Zn in the studied samples are greater than the ones corresponding to other metals. So, it is not strange to find Zn linked to all the fractions, even

**Table 2**
Concentration of metals (±confidence interval, $n = 4$, $\alpha = 0.05$) in mg kg$^{-1}$ (dry basis) for fractionation Scheme 2.

| | Cd | Cr | Cu | Ni | Pb | Zn |
|---|---|---|---|---|---|---|
| Fraction 1 (step 1) | | | | | | |
| S1 | 0.63 ± 0.05 | <0.65 | 14.84 ± 0.65 | <0.65 | 3.35 ± 0.31 | 109 ± 8 |
| S2 | 0.63 ± 0.05 | <0.65 | 5.43 ± 0.22 | <0.65 | 5.85 ± 0.53 | 53.50 ± 4.65 |
| S3 | 0.72 ± 0.06 | <0.65 | 6.33 ± 0.24 | 3.12 ± 0.22 | 4.98 ± 0.47 | 23.12 ± 2.07 |
| S4 | 0.50 ± 0.04 | <0.65 | 14.02 ± 0.62 | <0.65 | 4.98 ± 0.44 | 43.12 ± 4.02 |
| S5 | 1.53 ± 0.11 | <0.65 | 8.78 ± 0.50 | 4.13 ± 0.38 | 3.05 ± 0.28 | 14.58 ± 1.18 |
| S6 | 0.95 ± 0.08 | <0.65 | 5.83 ± 0.53 | 3.00 ± 0.24 | <1.70 | 50.15 ± 4.73 |
| S7 | 1.10 ± 0.09 | <0.65 | <0.75 | <0.65 | 6.98 ± 0.61 | 13.73 ± 1.06 |
| S8 | 0.69 ± 0.06 | <0.65 | 12.84 ± 0.37 | <0.65 | <1.70 | 129 ± 11 |
| MURST-ISS-A1 | 0.51 ± 0.04 | <0.65 | <0.75 | <0.65 | <1.70 | 7.15 ± 0.58 |
| Fraction 2 (step 2) | | | | | | |
| S1 | 0.25 ± 0.02 | 2.85 ± 0.23 | 2.10 ± 0.18 | 4.95 ± 0.45 | 4.88 ± 0.42 | 83.50 ± 5.23 |
| S2 | 0.30 ± 0.03 | 1.75 ± 0.15 | 4.73 ± 0.35 | 3.33 ± 0.30 | 6.83 ± 0.61 | 12.55 ± 1.06 |
| S3 | 1.02 ± 0.07 | 4.33 ± 0.38 | 10.10 ± 0.98 | 6.03 ± 0.57 | 12.35 ± 1.03 | 19.65 ± 1.72 |
| S4 | 0.25 ± 0.03 | 2.65 ± 0.20 | 8.35 ± 0.73 | 7.33 ± 0.69 | 8.95 ± 0.75 | 13.05 ± 1.13 |
| S5 | 0.36 ± 0.04 | <0.65 | 10.98 ± 0.95 | 6.52 ± 0.61 | 18.33 ± 1.63 | 23.33 ± 2.02 |
| S6 | 1.05 ± 0.10 | 5.00 ± 0.42 | 12.55 ± 1.02 | 7.13 ± 0.65 | 4.30 ± 0.39 | 21.03 ± 1.95 |
| S7 | 0.78 ± 0.07 | 4.13 ± 0.36 | 8.58 ± 0.69 | 2.98 ± 0.25 | 11.85 ± 1.05 | 9.25 ± 0.68 |
| S8 | 0.25 ± 0.02 | <0.65 | 2.10 ± 0.20 | <0.65 | <1.70 | 163 ± 14 |
| MURST-ISS-A1 | <0.10 | <0.65 | <0.75 | <0.65 | <1.70 | 1.63 ± 0.15 |
| Fraction 3 (step 3) | | | | | | |
| S1 | 0.70 ± 0.06 | 4.80 ± 0.35 | 5.25 ± 0.46 | 4.75 ± 0.42 | 13.75 ± 1.15 | 41.36 ± 3.75 |
| S2 | 0.75 ± 0.07 | 6.19 ± 0.57 | 13.51 ± 1.12 | 12.45 ± 1.03 | 29.39 ± 2.35 | 54.75 ± 4.22 |
| S3 | 0.63 ± 0.05 | 16.43 ± 1.46 | 15.75 ± 1.07 | 8.93 ± 0.71 | 9.45 ± 0.85 | 42.13 ± 3.66 |
| S4 | 0.96 ± 0.09 | 15.63 ± 1.39 | 14.15 ± 1.22 | 8.22 ± 0.65 | 35.83 ± 3.12 | 67.38 ± 5.85 |
| S5 | 0.73 ± 0.06 | 14.53 ± 1.18 | 24.22 ± 2.03 | 6.38 ± 0.55 | 19.92 ± 1.75 | 42.10 ± 3.78 |
| S6 | 0.86 ± 0.08 | 15.85 ± 1.24 | 25.15 ± 2.05 | 9.65 ± 0.72 | 20.73 ± 1.98 | 58.12 ± 4.25 |
| S7 | <0.10 | <0.65 | 4.05 ± 0.33 | 2.83 ± 0.25 | 17.63 ± 1.65 | 42.55 ± 3.95 |
| S8 | <0.10 | 8.80 ± 0.52 | 9.04 ± 0.48 | 6.45 ± 0.48 | 6.17 ± 0.50 | 41.36 ± 3.55 |
| MURST-ISS-A1 | <0.10 | <0.65 | <0.75 | 0.75 ± 0.06 | <1.70 | <0.05 |
| Fraction 4 (step 4) | | | | | | |
| S1 | 0.58 ± 0.02 | 11.16 ± 1.05 | 45.37 ± 4.02 | 5.15 ± 0.43 | 15.05 ± 1.33 | 93.88 ± 8.15 |
| S2 | 0.50 ± 0.04 | 16.56 ± 1.33 | 25.22 ± 2.13 | 10.05 ± 0.92 | 15.71 ± 1.39 | 61.25 ± 5.02 |
| S3 | 0.63 ± 0.05 | 8.33 ± 0.72 | 27.75 ± 2.35 | 4.63 ± 0.42 | 8.95 ± 0.75 | 16.13 ± 1.33 |
| S4 | 0.72 ± 0.05 | 8.65 ± 0.81 | 27.07 ± 2.08 | 8.44 ± 0.75 | 13.22 ± 1.05 | 17.43 ± 1.05 |
| S5 | 0.63 ± 0.04 | 12.22 ± 1.03 | 20.13 ± 1.66 | 9.15 ± 0.83 | 12.15 ± 0.99 | 25.95 ± 1.98 |
| S6 | 0.63 ± 0.05 | 12.25 ± 0.98 | 10.45 ± 0.78 | 8.02 ± 0.68 | 6.05 ± 0.41 | 13.75 ± 1.08 |
| S7 | 0.62 ± 0.04 | <0.65 | 26.08 ± 2.23 | <0.65 | 16.96 ± 1.25 | 6.54 ± 0.45 |
| S8 | <0.10 | 11.16 ± 1.05 | 50.37 ± 4.02 | 5.33 ± 0.42 | 15.05 ± 1.03 | 194 ± 14 |
| MURST-ISS-A1 | <0.10 | 2.25 ± 0.19 | 4.18 ± 0.29 | 3.02 ± 0.28 | <1.70 | 4.73 ± 0.52 |
| Fraction 5 (step 5) | | | | | | |
| S1 | 1.10 ± 0.09 | 15.98 ± 1.25 | 21.63 ± 1.83 | 17.25 ± 1.33 | 15.36 ± 1.22 | 61.00 ± 5.08 |
| S2 | 1.26 ± 0.11 | 16.13 ± 1.32 | 29.17 ± 2.35 | 16.05 ± 1.45 | 16.12 ± 1.30 | 50.02 ± 4.30 |
| S3 | 0.83 ± 0.08 | 11.12 ± 1.03 | 20.45 ± 2.02 | 14.24 ± 1.12 | 12.05 ± 1.11 | 40.35 ± 3.98 |
| S4 | 1.43 ± 0.13 | 13.85 ± 1.09 | 29.63 ± 2.11 | 21.25 ± 1.58 | 11.25 ± 0.98 | 49.05 ± 4.12 |
| S5 | 1.10 ± 0.08 | 26.28 ± 2.02 | 40.63 ± 3.28 | 17.13 ± 1.33 | 25.12 ± 2.07 | 61.38 ± 5.05 |
| S6 | 1.55 ± 0.13 | 27.12 ± 2.15 | 19.93 ± 1.55 | 19.75 ± 1.42 | 14.42 ± 1.28 | 79.85 ± 6.33 |
| S7 | 0.67 ± 0.06 | 10.92 ± 1.04 | 37.76 ± 2.33 | 16.33 ± 1.38 | 16.15 ± 1.36 | 23.56 ± 1.45 |
| S8 | 0.28 ± 0.03 | 13.80 ± 1.12 | 22.63 ± 1.24 | 14.75 ± 1.06 | 4.36 ± 0.31 | 31.00 ± 2.81 |
| MURST-ISS-A1 | <0.10 | 41.33 ± 3.75 | 2.45 ± 0.13 | 5.95 ± 0.35 | 18.02 ± 1.63 | 41.15 ± 3.63 |

to the organic matter fraction. Other authors have found the same behaviour for Zn in samples with high content of organic matter [36].

The Factor 3 vs. Factor 2 plot distributes the metals in three quadrants (Fig. 5e). Cr and Ni have positive values for Factor 3 and negative for Factor 2 and they could be related to the more unavailable fractions, i.e. crystalline oxide and residual phases. A close inspection Tables 1 and 2 demonstrates that F3 and F5 have a Cr average value higher than 50% of the total Cr content. Moreover, Cr is not present in F1, indicating that this metal is mainly linked to the unavailable fractions. A lower value of Factor 3 was observed for Ni. This fact could be ascribed to a higher relative abundance of this metal in the amorphous oxide phase (F2) compared to the crystalline one (F3). Cd appears with negative values for both Factors 2 and 3. This may be due to a higher proportion of this metal in the available or labile phases (F1). Although Pb is also in the same quadrant, the relationship 'Cd in F1/total Cd' is higher than the corresponding ratio for Pb. This is appreciated as a more negative value for Factor 3. Again, Factor 2 allows Cu and Zn to be distinguished from the other metals, probably because of their association with organic matter, as we have already pointed out.

Factor 1 and Factor 3 could be simultaneously analyzed in Fig. 5f. Three clusters could be observed. One of them involves Zn and Cd with lower values for Factor 1, the other comprises Pb and Cu and the third group includes Cr and Ni with positive values for both Factor 3 and Factor 1. The combination of these two factors seems to be related with mobility/availability of metals. Cd and Zn exhibit the higher mobility whereas Ni and Cr are the less available metals, that it is consistent with reports by other authors [36]. An intermediate situation is observed for Pb and Cu, which exhibit similar mobility. Mobility/availability of metals is strongly related to the geochemical composition of the sediments and also to the characteristics of the environment in which the sediments are located. However, several studies applied to different oxic sediments samples reported a similar sequence of mobility/availability. In this sense, Zakir et al. [18] established the sequence Cd > Zn > Pb > Cu > Cr for surface sediments and Sahuquillo et al. [37] reported the order Cd > Zn > Pb ≈ Cu > Ni ≈ Cr


**Fig. 3.** Distribution pattern—bar diagram.

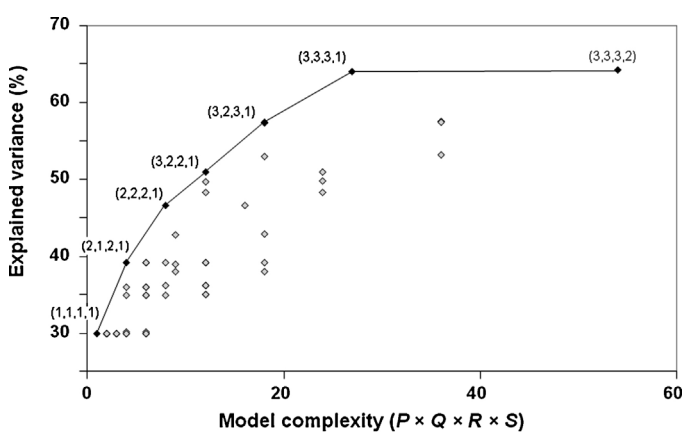


**Fig. 4.** Explained data variance (%) by Tucker4 models of different complexity.

for the relative mobilization of metals in different sediment samples. On the contrary, other authors reported different sequences; Forghani et al. [38] informed the following trend in the mobility: Cd > Pb > Zn > Ni, whereas Cr and Cu appeared as environmentally immobile. On the other hand, Canuto et al. [39] stated that the order of mobility is Cd > Pb > Zn > Ni ≈ Cr > Cu for polluted estuarine sediments. The main differences among the mobility order observed in our study and the reported ones in the last studies [38,39] are the unavailability of Cu and some variations in the relative mobility of Pb.

*K*-mode (fractions) loading plots are depicted in Fig. 5g–i. Factor 2 vs. Factor 1 graph shows that all fractions have similar positive values for Factor 2, except F4 (organic matter fraction) which has the more positive loading (Fig. 5g). The relationship between Factor 2 and F4 has been a common issue throughout the discussion of all the modes (samples, metals and fractions). The loading distribution along Factor 1 passes from negative to positive values in agreement with the fraction availability (i.e. the more negative the loadings are, the more available the fractions are). In this loading plot, it can be observed that F4 is in the neighbourhood of F2 (amorphous oxides of Fe and Mn). This fact could be explained in terms of the natural association of these phases. In this sense, organic matter usually acts as a coating of oxide particles. Moreover, amorphous oxides often form aggregates that occlude organic matter.

The Factor 3 vs. Factor 2 plot shows that F4 is separated from the other fractions with positive values for both Factors 2 and 3 (Fig. 5h). On the other hand, the oxide phases (F2 and F3) appear together. This is consistent with several classical extraction schemes [6,9], in which the amorphous and crystalline oxides were encompassed in a unique fraction.

Three well-defined groups are defined in Factor 3 vs. Factor 1 plot (Fig. 5i). F4 (organic matter) appears isolated. F1 and F2 (i.e. the more available/labile phases) are grouped with negative values for both Factors 1 and 3. On the other side, F3 and F5 (representing the crystalline oxide and residual phases) have negative values for Factor 3 and positive ones for Factor 1. Therefore, this distribution seems to obey to the ability of each phase to retain the metals associated to them.

A single factor was recovered by Tucker4 model for the *L*-mode (sequential extraction schemes). The loading values are almost the same for both sequential schemes (approximately 0.7). Although the sequential extraction schemes involve different number and order of extraction steps (Fig. 2) as well as different reagents, extraction times and temperature, they have quite similar loading values. This could be assigned to the resemblance among the information obtained by the two schemes studied.

Table 5 shows the most important elements of the core array **G** obtained by the Tucker4 model with complexity 3 × 3 × 3 × 1. The

**Table 3**
Comparison between total metal concentrations and the sum of fractions. Concentration of metals (±confidence interval, $n = 4$, $\alpha = 0.05$) in mg kg$^{-1}$ (dry basis).

| Sample | | Cd | Cr | Cu | Ni | Pb | Zn |
|---|---|---|---|---|---|---|---|
| S1 | Total concentration | 3.18 ± 0.10 | 36.22 ± 1.33 | 87.28 ± 3.72 | 31.12 ± 1.36 | 50.35 ± 3.93 | 386 ± 14 |
| | $\sum$ fractions Scheme 1 | 3.13 ± 0.10 | 34.43 ± 1.57 | 83.26 ± 3.81 | 29.67 ± 1.42 | 51.48 ± 2.29 | 392 ± 14 |
| | Recovery* (%) | **98.4** | **95.1** | **95.4** | **95.3** | **102.2** | **101.6** |
| | $\sum$ fractions Scheme 2 | 3.26 ± 0.12 | 34.79 ± 1.69 | 89.19 ± 4.49 | 32.10 ± 1.53 | 52.39 ± 2.20 | 388 ± 14 |
| | Recovery (%) | **102.5** | **96.1** | **102.2** | **103.1** | **104.1** | **100.6** |
| S2 | Total concentration | 3.36 ± 0.11 | 40.02 ± 2.05 | 76.75 ± 3.12 | 40.15 ± 2.13 | 70.13 ± 3.75 | 230 ± 10 |
| | $\sum$ fractions Scheme 1 | 3.29 ± 0.11 | 36.02 ± 1.65 | 74.55 ± 3.23 | 38.15 ± 1.72 | 65.79 ± 3.06 | 218 ± 9 |
| | Recovery (%) | **98.0** | **90.0** | **97.1** | **95.0** | **93.8** | **94.5** |
| | $\sum$ fractions Scheme 2 | 3.44 ± 0.15 | 40.63 ± 1.96 | 78.06 ± 3.39 | 41.88 ± 2.02 | 73.90 ± 3.13 | 232 ± 9 |
| | Recovery (%) | **102.4** | **101.5** | **101.7** | **104.3** | **105.4** | **100.8** |
| S3 | Total concentration | 3.78 ± 0.12 | 39.95 ± 1.89 | 81.44 ± 3.22 | 36.02 ± 1.65 | 46.32 ± 1.98 | 141 ± 9 |
| | $\sum$ fractions Scheme 1 | 3.77 ± 0.13 | 36.92 ± 1.73 | 78.73 ± 3.09 | 34.25 ± 1.43 | 46.35 ± 1.86 | 138 ± 6 |
| | Recovery (%) | **99.7** | **92.4** | **96.7** | **95.1** | **100.1** | **98.0** |
| | $\sum$ fractions Scheme 2 | 3.83 ± 0.14 | 40.21 ± 1.96 | 80.38 ± 3.43 | 36.95 ± 1.52 | 47.78 ± 1.95 | 141 ± 6 |
| | Recovery (%) | **101.3** | **100.7** | **98.7** | **102.6** | **103.2** | **100.5** |
| S4 | Total concentration | 3.72 ± 0.11 | 39.85 ± 1.72 | 90.88 ± 3.11 | 44.87 ± 2.58 | 75.36 ± 4.03 | 191 ± 10 |
| | $\sum$ fractions Scheme 1 | 3.51 ± 0.14 | 39.98 ± 1.90 | 86.10 ± 3.44 | 45.86 ± 2.18 | 71.15 ± 3.50 | 186 ± 8 |
| | Recovery (%) | **94.4** | **100.3** | **94.7** | **102.2** | **94.4** | **97.5** |
| | $\sum$ fractions Scheme 2 | 3.86 ± 0.17 | 40.78 ± 1.95 | 93.22 ± 3.29 | 45.24 ± 1.99 | 74.23 ± 3.54 | 190 ± 8 |
| | Recovery (%) | **103.8** | **102.3** | **102.6** | **100.8** | **98.5** | **99.8** |
| S5 | Total concentration | 4.12 ± 0.13 | 52.02 ± 2.32 | 103 ±4 | 40.12 ± 1.73 | 78.95 ± 4.27 | 166 ± 9 |
| | $\sum$ fractions Scheme 1 | 4.02 ± 0.12 | 48.17 ± 2.66 | 102 ± 5 | 40. 60 ± 1.55 | 77.43 ± 3.42 | 162 ± 7 |
| | Recovery (%) | **97.6** | **92.6** | **99.6** | **101.2** | **98.1** | **97.6** |
| | $\sum$ fractions Scheme 2 | 4.35 ± 0.16 | 53.03 ± 2.56 | 105 ± 4 | 43.31 ± 1.79 | 78.57 ± 3.33 | 167 ± 7 |
| | Recovery (%) | **105.6** | **101.9** | **102.2** | **108.0** | **99.5** | **100.9** |
| S6 | Total concentration | 4.96 ± 0.18 | 57.45 ± 2.53 | 74.85 ± 3.55 | 46.01 ± 1.82 | 42.37 ± 2.14 | 225 ±11 |
| | $\sum$ fractions Scheme 1 | 4.86 ± 0.17 | 54.39 ± 2.73 | 76.97 ± 2.99 | 44.93 ± 1.78 | 41.64 ± 2.17 | 233 ± 10 |
| | Recovery (%) | **98.0** | **94.7** | **102.8** | **97.7** | **98.3** | **103.4** |
| | $\sum$ fractions Scheme 2 | 5.04 ± 0.21 | 60.22 ± 2.70 | 73.91 ± 2.92 | 47.55 ± 1.86 | 45. 50 ± 2.42 | 223 ± 9 |
| | Recovery (%) | **101.6** | **104.8** | **98.7** | **103.3** | **107.4** | **99.1** |
| S7 | Total concentration | 3.33 ± 0.12 | 17.08 ± 0.92 | 77.25 ± 3.62 | 24.48 ± 1.21 | 70.65 ± 3.99 | 97.33 ±6.48 |
| | $\sum$ fractions Scheme 1 | 3.24 ± 0.13 | 18.13 ± 1.10 | 75.80 ± 3.51 | 21.06 ± 1.15 | 70.94 ± 2.95 | 97.29 ± 4.69 |
| | Recovery (%) | **97.3** | **106.1** | **98.1** | **86.0** | **100.4** | **100.0** |
| | $\sum$ fractions Scheme 2 | 3.37 ± 0.13 | 15.05 ± 1.10 | 76.47 ± 3.31 | 22.14 ± 1.42 | 69.57 ± 2.76 | 95.63 ± 4.42 |
| | Recovery (%) | **101.2** | **88.1** | **99.0** | **90.4** | **98.5** | **98.3** |
| S8 | Total concentration | 1.25 ± 0.05 | 34.13 ± 1.74 | 97.88 ± 3.86 | 27.15 ± 1.29 | 24.56 ± 1.45 | 561 ± 20 |
| | $\sum$ fractions Scheme 1 | 1.19 ± 0.07 | 32.54 ± 1.74 | 97.26 ± 5.09 | 25.81 ± 1.24 | 25.40 ± 1.37 | 538 ± 21 |
| | Recovery (%) | **95.2** | **95.3** | **99.4** | **95.1** | **103.4** | **95.8** |
| | $\sum$ fractions Scheme 2 | 1.22 ± 0.07 | 33.76 ± 1.62 | 96.98 ± 4.26 | 26.53 ± 1.24 | 25.58 ± 1.19 | 558 ± 23 |
| | Recovery (%) | **97.6** | **98.9** | **99.1** | **97.7** | **104.2** | **99.4** |
| MURST-ISS-A1 | Total concentration | 0.53 ± 0.03 | 43.85 ± 2.68 | 6.08 ± 0.38 | 9.12 ± 0.55 | 18.45 ± 1.02 | 57.12 ± 2.98 |
| | $\sum$ fractions Scheme 1 | 0.49 ± 0.04 | 43.02 ± 3.85 | 6.10 ± 0.42 | 9.81 ± 0.52 | 17.24 ± 1.58 | 53.16 ± 3.79 |
| | Recovery (%) | **92.5** | **98.1** | **100.3** | **107.6** | **93.4** | **93.1** |
| | $\sum$ fractions Scheme 2 | 0.51 ± 0.04 | 43.58 ± 3.75 | 6.63 ± 0.32 | 9.72 ± 0.45 | 18.02 ± 1.63 | 54.71 ± 3.72 |
| | Recovery (%) | **96.2** | **99.4** | **109.0** | **106.6** | **97.7** | **95.8** |
| | Certified value | 0.538 ± 0.027 | 42.1 ± 3.4 | 5.79 ± 1.59 | 9.56 ± 1.05 | 21.0 ± 2.9 | 53.3 ± 2.7 |

* Recovery is defined as 100 × (Σ fractions/(determined) total concentration).

**Table 4**
St-coefficients for the convex hull method results obtained for Tucker4 models of different complexity.

| Model complexity | d.f. | St-coefficient |
|---|---|---|
| (1,1,1,1) | 521 | – |
| (2,1,2,1) | 510 | 0.77 |
| (2,2,2,1) | 521 | 1.98 |
| (3,2,2,1) | 505 | 0.50 |
| (3,2,3,1) | 496 | 1.64 |
| (3,3,3,1) | 509 | 90.7 |
| (3,3,3,2) | 487 | – |

d.f.: degrees of freedom.

**Table 5**
Four most important core elements of the (3,3,3,1) Tucker4 model.

| Core element ($p \times q \times r \times s$) | Core element value | Explained variance (%) |
|---|---|---|
| [1,1,1,1] | −11.69 | 40.44 |
| [2,2,2,1] | 7.15 | 15.13 |
| [3,1,2,1] | −6.08 | 10.92 |
| [2,1,3,1] | 4.77 | 6.73 |

core elements $g_{pqrs}$ contain information regarding the extent of the interaction among the loading matrices $\mathbf{A}_p$, $\mathbf{B}_q$, $\mathbf{C}_r$ and $\mathbf{D}_s$ ($p = 1,2,3$; $q = 1,2,3$; $r = 1,2,3$ and $s = 1$). From Eq. (1) it may be noted that the sign of $g_{pqrs}$ is defined by the sign of $\mathbf{A}_p$, $\mathbf{B}_q$, $\mathbf{C}_r$ and $\mathbf{D}_s$. Moreover, the magnitude of each core value is related to its contribution to the reconstructed data (i.e. the product $a_{ip} \times b_{jq} \times c_{kr} \times d_{ls} \times g_{pqrs}$).

The first core element (1,1,1,1) explains a 40.44% of the core variation and indicates an interaction among the first factors in each mode ($A_1$, $B_1$, $C_1$ and $D_1$, i.e. the Factor 1 for the *I*, *J*, *K* and *L*-modes). This first core value is negative (−11.69), and loading values of $A_1$ are negative as well (see Fig. 5a). On the other hand, $B_1$ and $D_1$ evidence positive values. Therefore, the product will be negative only if the first core value interacts with the positive values of $C_1$. Additionally, the high value of this core element indicates a relationship between the more positive values of $B_1$ and $C_1$ and the more negative values of $A_1$. Thus, Ni, Cr and Cu will be related to the F5 (residual) and F3 (crystalline oxides) to a lesser extent. This is in accordance with the presence of these metals in such geochemical phases, as we have already mentioned. Likewise, the samples showing more negative values of $A_1$ are S5, MURST,

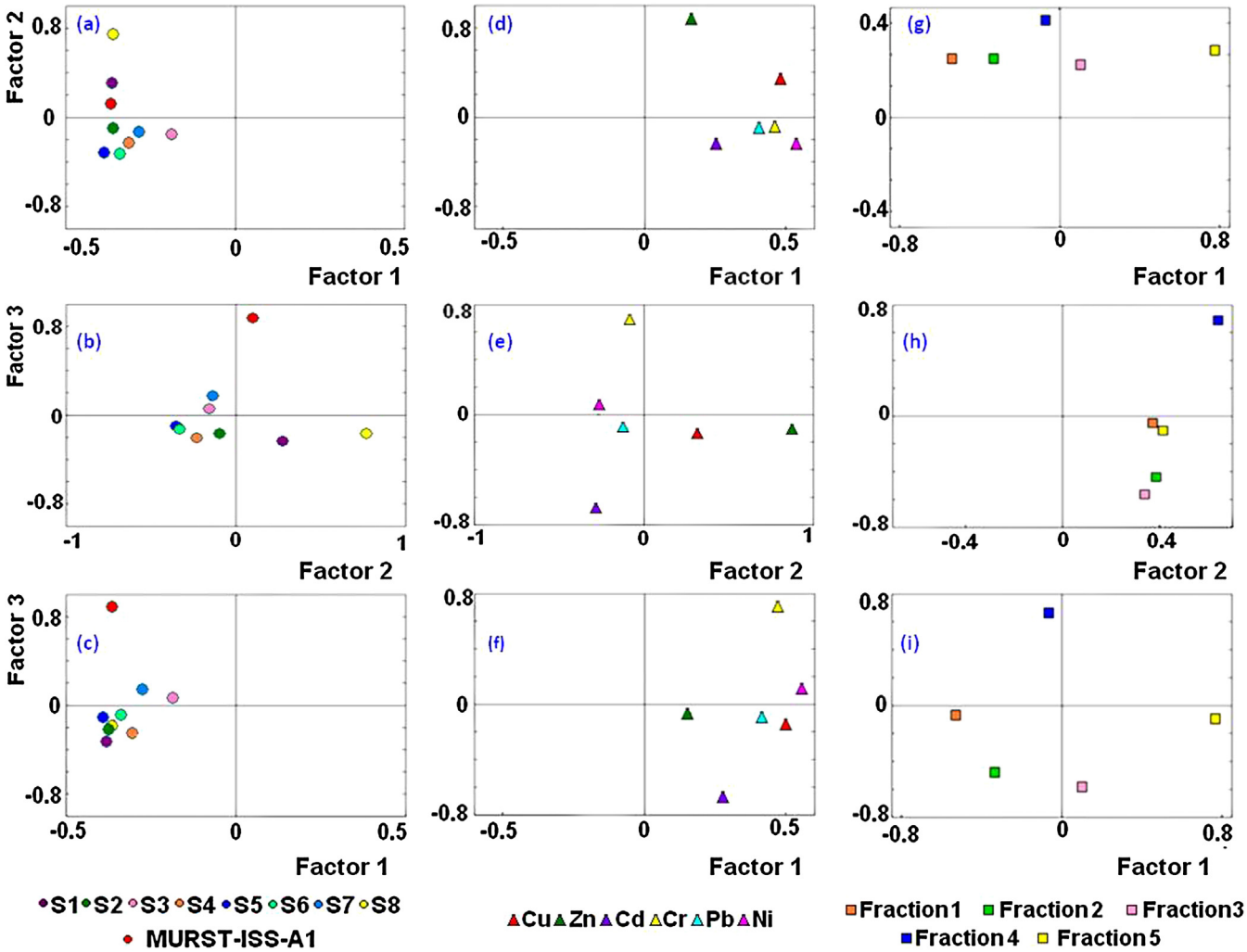


**Fig. 5.** (a)–(c) Loading plots for the *I*-mode (samples), (d)–(f) loading plots for the *J*-mode (metals) and (g)–(i) loading plots for the *K*-mode (fractions) obtained by Tucker4 model.

S1, S8 and S2. Nevertheless, the values are similar for most of the samples.

The second core element (2,2,2,1) has a positive value of 7.15 (15.13% explained core variability). Since $C_2$ and $D_1$ are always positive, obtaining a positive core value involves the product between negative values for $A_2$ and $B_2$ or between positive values for both $A_2$ and $B_2$. The samples having positive loading values in the *I*-mode are MURST, S1 and S8, and these samples would be related to Cu and Zn in the *J*-mode (also positive values). With respect to the samples having negative values in $A_2$ and the metals with negative values in $B_2$ it is not possible to distinguish a clear relationship. In the *K*-mode, the most positive value corresponds to F4 (organic matter), and this could be related to the presence of Cu and Zn in this fraction. This could also be associated with samples MURST, S1 and S8, which exhibit high proportions of Cu and Zn linked to organic matter fraction, as was already discussed.

The third core element (3,1,2,1) has a negative value (−6.08) and it explains a 10.92% of the core variation. Since $B_1$, $C_2$ and $D_1$ are always positive the core value will be negative if we consider negative values of $A_3$. Unfortunately, this core element is unable to show a clear relationship between samples, fractions and metals.

Finally, the fourth core element (2,1,3,1) has a positive value of 4.77 (6.73% explained core variability). Since $B_1$ and $D_1$ are always positive, obtaining a positive core value involves the product between negative values for both $A_2$ and $C_3$ or between positive values for $A_2$ and $C_3$. Thus, samples S1, S8 and MURST appear associated to F4 (organic matter) as was already stated. On the other hand, the most negative values of $C_3$ are for F2 and F3 (amorphous oxyhydroxides of Fe and Mn and crystalline oxides of Fe, respectively) and they could be related to samples S4, S5 and S6 (more negative loadings for $A_2$) and to the metals with more positive loading values in $B_1$ (i.e., Ni, Cr, Cu and Pb). Particularly, there is a significant proportion of Pb in the oxyhydroxide fraction for these samples (Fig. 3).

## 4. Conclusions

The mobility/availability of metals in sediment samples of the Bahía Blanca Estuary could be satisfactorily investigated by the combination of two different sequential extraction schemes and chemometric multivariate analysis. The application of the Tucker4 model to the data obtained enabled us to easily visualize and explain the information underlying in the data set.

Several conclusions about samples could be pointed out: two samples (S1 and S8) seem to be influenced by the proximity to industrial effluents. Consequently, higher proportions of metals linked to organic matter fraction are observed. In addition, other samples are characterized by relatively high contents of Pb in the oxyhydroxide fractions (S4, S5 and S6).

Regarding the metals, a few remarks can be made: Cd and Zn are associated to the more available fractions (F1 and F2). Ni, Cr, Cu and Pb are mainly associated to the unavailable fractions (F3 and F5). There is a tight relationship between Cu and Zn and the organic matter fraction.

The procedures applied in the two sequential extraction schemes differ in the number of steps, type of reagents used, and the order in which metals associated to organic matter is extracted. In spite of this, the visualization of the information extracted by Tucker4 model does not show significant differences among the two sequential extraction schemes. So, the information supplied by the two sequential extraction schemes could be considered equivalent.

From the multivariate analysis, it can be inferred that Factor 1 is strongly related to metal availability. The lower Factor 1 is the lesser the tendency of geochemical fractions to retain the metals (F1 < F2 < F4 < F3 < F5), i.e. the higher the metal availability (Cd ≈ Zn > Pb ≈ Cu > Ni > Cr). Else wise, Factor 2 could be assigned to the organic matter content, i.e. the contributions of anthropogenic origin to the sediments. Factor 3 it is probably the result of a combination of several causes. Therefore, it was not possible to clearly identify which characteristics describe it.

## Acknowledgements

Financial support from Universidad Nacional del Sur (24/Q032) is gratefully acknowledged. P. Y. Quintas, M. Garrido and B. S. Fernández Band whish to thank Consejo Nacional de Investigaciones Científicas y Técnicas (CONICET).

## References

[1] S.K. Sundaray, B.B. Nayak, S. Lin, D. Bhatta, Geochemical speciation and risk assessment of heavy metals in the river estuarine sediments—a case study: Mahanadi basin, India, J. Hazard. Mater. 186 (2011) 1837–1846.
[2] M.B. Arain, T.G. Kazi, M.K. Jamali, N. Jalbani, H.I. Afridi, J.A. Baig, Speciation of heavy metals in sediment by conventional, ultrasound and microwave assisted single extraction methods: a comparison with modified sequential extraction procedure, J. Hazard. Mater. 154 (2008) 998–1006.
[3] J.E. Fergusson, The Heavy Elements: Chemistry, Environmental Impact and Health Effects, Pergamon Press, New York, NY, 1990.
[4] K.M. Mohiuddin, Y. Ogawa, H.M. Zakir, K. Otomo, N. Shikazono, Heavy metals contamination in water and sediments of an urban river in a developing country, Int. J. Environ. Sci. Technol. 8 (2011) 723–736.
[5] R. Arias, A. Barona, G. Ibarra-Berastegi, I. Aranguiz, A. Elías, Assessment of metal contamination in dregded sediments using fractionation and Self-Organizing Maps, J. Hazard. Mater. 151 (2008) 78–85.
[6] Ph. Quevauvillier, Operationally defined extraction procedures for soil and sediment analysis I. Standardization, TrAC, Trends Anal. Chem. 17 (1998) 289–298.
[7] D.M. Templeton, F. Ariese, R. Cornelis, L.G. Danielsson, H. Muntau, H.P. Van Leeuwen, R. Lobinski, Guidelines for terms related to chemical speciation and fractionation of elements. Definitions, structural aspects, and methodological approaches (IUPAC recommendations 2000), Pure Appl. Chem. 72 (2000) 1453–1470.
[8] G. Rauret, Extraction procedures for the determination of heavy metals in contaminated soil and sediment, Talanta 46 (1998) 449–455.
[9] A. Tessier, P.S.C. Campbell, M. Bisson, Sequential extraction procedure for the speciation of particulate trace metals, Anal. Chem. 51 (1979) 844–851.
[10] S.K. Gupta, K.Y. Chen, Partitioning of trace metals in selective chemical fractions of nearshore sediments, Environ. Lett. 10 (1975) 129–158.
[11] G.E.M. Hall, G. Gauthier, J.C. Pelchat, P. Pelchat, J.E. Vaive, Application of a sequential extraction scheme to ten geological certified reference materials for the determination of 20 elements, J. Anal. Atom. Spectrom. 11 (1996) 787–796.
[12] G. Rauret, J.F. López-Sánchez, A. Sahuquillo, R. Rubio, C. Davidson, A. Ure, Ph. Quevauviller, Improvement of the BCR three step sequential extraction procedure prior to the certification of new sediment and soil reference materials, J. Environ. Monit. 1 (1999) 57–61.
[13] K. Nemati, N.K.A. Bakar, M.R. Abas, E. Sobhanzadeh, Speciation of heavy metals by modified BCR sequential extraction procedure in different depths of sediments from Sungai Buloh, Selangor, Malaysia, J. Hazard. Mater. 192 (2011) 402–410.
[14] M.L. Silveira, L.R.F. Alleoni, G.A. O'connor, A.C. Chang, Heavy metal sequential extraction methods—a modification for tropical soils, Chemosphere 64 (2006) 1929–1938.
[15] E. Torres, M. Auleda, A sequential extraction procedure for sediments affected by acid mine drainage, J. Geochem. Explor. 128 (2013) 35–41.
[16] S.M. Sakan, N.M. Sakan, D.S. Dordević, Trace element study in Tisa River and Danube alluvial sediment in Serbia, Int. J. Sediment Res. 28 (2013) 234–245.
[17] F.X. Han, W. Kingery, J.E. Hargreaves, T.W. Walker, Effects of land uses on solid-phase distribution of micronutrients in selected vertisols of the Mississippi River Delta, Geoderma 142 (2007) 96–103.
[18] H.M. Zakir, N. Shikazono, K. Otomo, Geochemical distribution of trace metals and assessment of anthropogenic pollution in sediments of Old Nakagawa River, Tokyo, Japan, Am. J. Environ. Sci. 4 (2008) 654–665.
[19] M.S. Masoud, T.O. Said, G.E. Zokm, M.A. Shreadah, Speciation of Fe, Mn and Zn in surficial sediments from the Egyptian Red Sea coasts, Chem. Speciation Bioavailability 22 (2010) 257–269.
[20] T.T. Chao, Selective dissolution of manganese oxides from soils and sediments with acidified hydroxylamine hydrochloride, Soil Sci. Soc. Am. J. 36 (1972) 764–768.
[21] W.F. Pickering, Metal ion speciation—soils and sediments (a review), Ore Geol. Rev. 1 (1986) 83–146.
[22] V.A. Guinder, C.A. Popovich, G.M.E. Perillo, Particulate suspended matter concentrations in the Bahía Blanca Estuary, Argentina: implication for the development of phytoplankton blooms, Estuarine Coastal Shelf Sci. 85 (2009) 157–165.
[23] S.E. Botté, R.H. Freije, J.E. Marcovecchio, Distribution of several heavy metals in tidal flats sediments within Bahía Blanca Estuary (Argentina), Water Air Soil Pollut. 210 (2010) 371–388.
[24] K.P. Singh, A. Malik, N. Basant, V.K. Singh, A. Basant, Multi-way data modeling of heavy metal fractionation in sediments from Gomti River (India), Chemom. Intell. Lab. Syst. 87 (2007) 185–193.
[25] I. Stanimirova, A. Kita, E. Malkowski, E. John, B. Walczak, N-way exploration of environmental data obtained from sequential extraction procedure, Chemom. Intell. Lab. Syst. 96 (2009) 203–209.
[26] M.B. Alvarez, M. Garrido, A.G. Lista, B.S. Fernández Band, Three-way multivariate analysis of metal fractionation results from sediment samples obtained by different sequential extraction procedures and ICP-OES, Anal. Chim. Acta 620 (2008) 34–43.
[27] M.B. Alvarez, C.E. Domini, M. Garrido, A.G. Lista, B.S. Fernández Band, Single-step chemical extraction procedures and chemometrics for assessment of heavy metal behaviour in sediment samples from the Bahía Blanca estuary, Argentina, J. Soils Sediments 11 (2011) 657–666.
[28] R. Pardo, B.A. Helena, C. Cazurro, C. Guerra, L. Debán, C.M. Guerra, M. Vega, Application of two- and three-way principal component analysis to the interpretation of chemical fractionation results obtained by the use of the B.C.R. procedure, Anal. Chim. Acta 523 (2004) 125–132.
[29] R. Bro, Review on multiway analysis in chemistry—2000–2005, Crit. Rev. Anal. Chem. 36 (2006) 279–293.
[30] R. Bro, Multi-way analysis in the food industry: models, algorithms, and applications, in: Ph.D. Thesis, University of Amsterdam, Amsterdam, 1998.
[31] M.B. Alvarez, M.E. Malla, D.A. Batistoni, Comparative assessment of two sequential chemical extraction schemes for the fractionation of Cd, chromium, lead and zinc in surface coastal sediments, Fresenius J. Anal. Chem. 369 (2001) 81–90.
[32] R. Rubio, A.M. Ure, Approaches to sampling and sample pretreatments for metal speciation in soils and sediments, Intern. J. Environ. Anal. Chem. 51 (1993) 205–217.
[33] E. Ceulemans, H.K.L. Kiers, Selecting among three-mode principal component models of different types and complexities: a numerical convex hull based method, Br. J. Math. Stat. Psychol. 56 (2006) 133–150.
[34] P.M. Kroonenberg, Applied Multiway Data Analysis, Wiley-Interscience, Hoboken, NJ, 2008.
[35] R. Bro, C.A. Anderson, N-way Toolbox for MATLAB (TM), 2013, ⟨http://www.models.life.ku.dk/nwaytoolbox/download⟩.
[36] J. Morillo, J. Usero, I. Gracia, Heavy metal distribution in marine sediments from the southwest coast of Spain, Chemosphere 55 (2004) 431–442.
[37] A. Sahuquillo, A. Rigol, G. Rauret, Overview of the use of leaching/extraction tests for risk assessment of trace metals in contaminated soils and sediments, TrAC, Trend. Anal. Chem. 22 (2003) 152–159.
[38] G. Forghani, F. Moore, A. Qishlaqi, The concentration and partitioning of heavy metals in surface sediments of the Maharlu Lake, SW Iran, Soil Sediment Contam. 21 (2012) 872–888.
[39] F.A.B. Canuto, C.A.B. Garcia, J.P.H. Alves, E.A. Passos, Mobility and ecological risk assessment of trace metals in polluted estuarine sediments using a sequential extraction scheme, Environ. Monit. Assess. 185 (2013) 6173–6185.